Electronic Supplementary Material (ESI) for Polymer Chemistry.

Designed incorporation of semi-crystalline domains into structured latex particles via solvent-aided emulsion polymerization

Adrián Perez, Emily Kynaston, Christopher Lindsay, Nicholas Ballard*

SUPPORTING INFORMATION

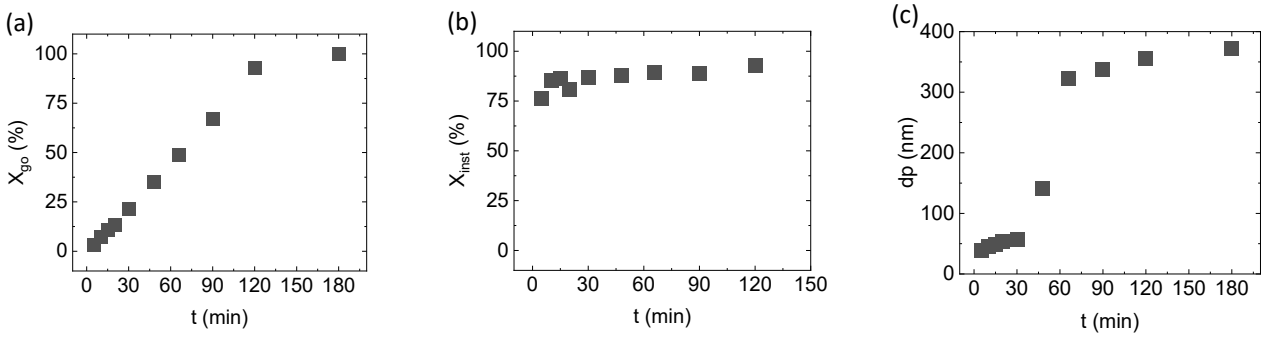

Figure S1. Evolution of conversion and particle size for semibatch emulsion polymerization of SA (reaction R7) under monomer starved conditions. (a) Global conversion. (b) Instantaneous conversion. (c) Particle size evolution.

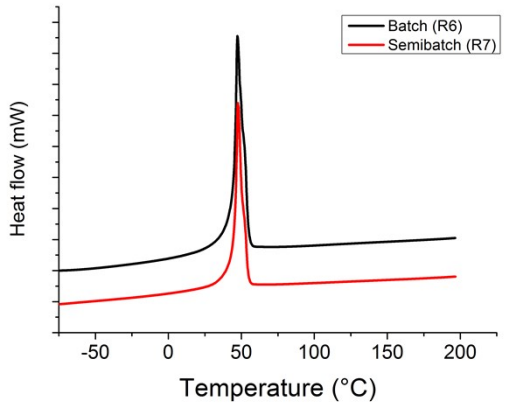

Figure S2. DSC thermograms of dried samples of semicrystalline latexes of poly(stearyl acrylate) synthesized in batch (R6) and in semibatch (R7).

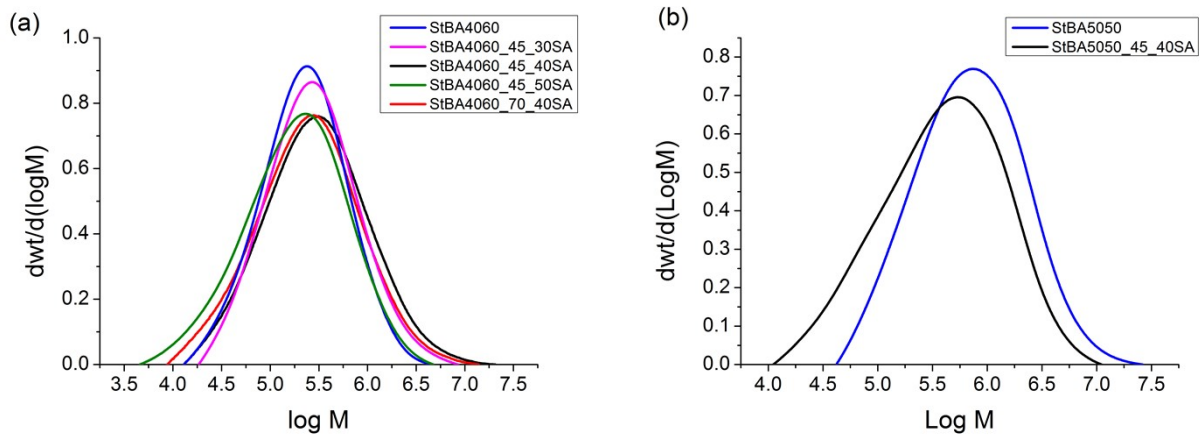

Figure S3. Molecular weight distributions measured by GPC of the different latexes synthesized in this work.

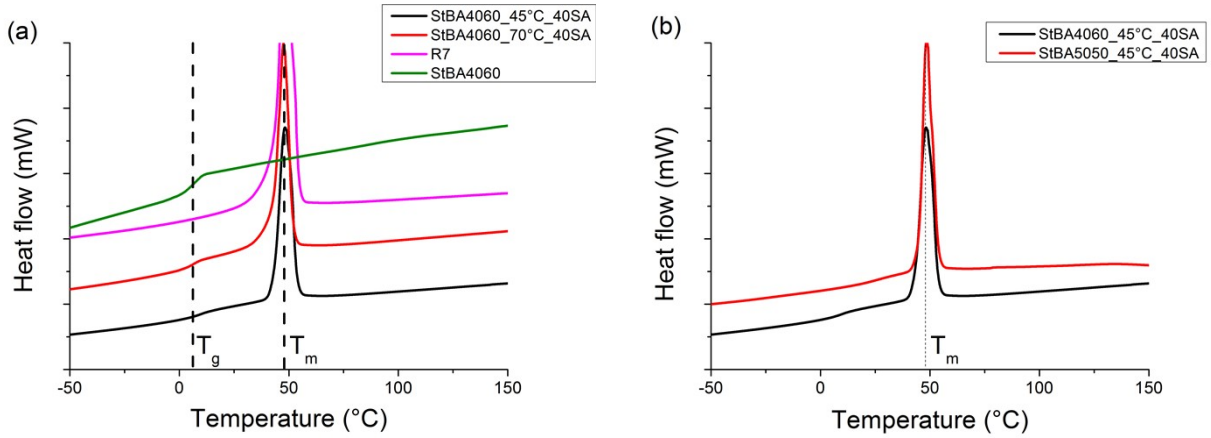

Figure S4. DSC thermograms of dried samples of semi-crystalline-amorphous hybrid latexes synthesized in this work. In (a) the results of the StBA4060 seed latex, a poly(stearyl acrylate) latex synthesized by semibatch emulsion polymerization (R7) and two hybrid latexes with 40% stearyl acrylate content are shown. In (b) the results for two latexes that have different initial seeds, either St:BA 40:60 or St:BA 50:50, are shown.

Table S1. Young's modulus (E), yield stress (σ_y), stress at break (σ_{max}), elongation at break (ε_{max}) and toughness obtained from corresponding to the tensile stress−strain plots represented in **Figure 5**.

Sample	E (MPa)	σ_y (MPa)	σ_{max} (MPa)	ε_{max}	Toughness (MPa)
StBA4060	1 ± 1	0.23 ± 0.49	*	*	*
CS	5 ± 1	0.79 ± 0.03	0.88 ± 0.08	5.71 ± 0.29	5.42 ± 0.17
StBA4060_45°C_40%pSA	36 ± 2	1.50 ± 0.01	1.60 ± 0.07	7.71 ± 1.27	11.40 ± 1.95
StBA4060_70°C_40%pSA	14 ± 3	0.80 ± 0.08	0.49 ± 0.38	10.43 ± 1.13	7.66 ± 0.61

*No sample breakage in the experimental strain range.

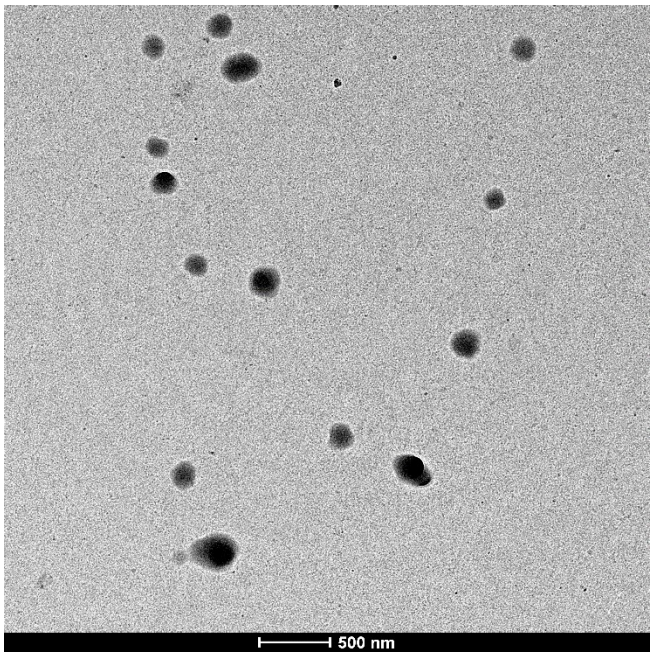

Figure S5. TEM images of reference core-shell latex particles (CS). Note that these latexes were not stained and therefore the color of the phases is inverted compared to the images in the main paper (semicrystalline phase is dark and amorphous phase is lighter).

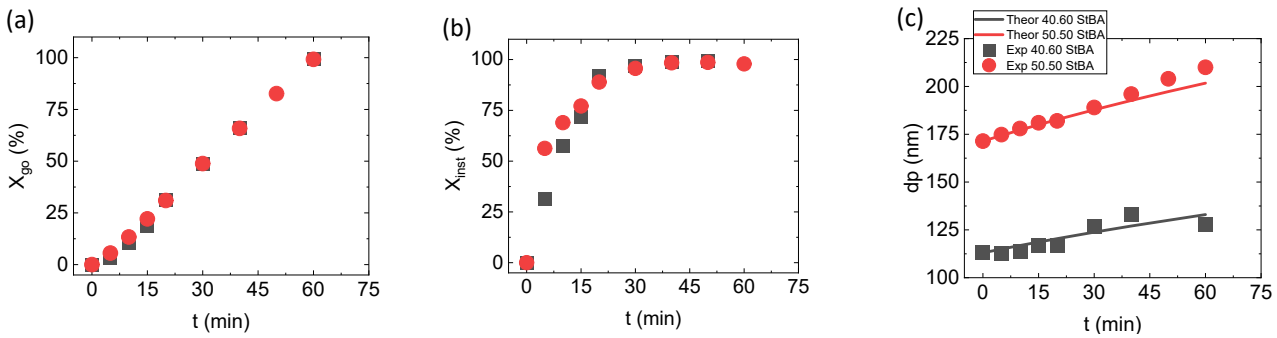

Figure S6. Evolution of conversion and particle size for seeded semibatch emulsion polymerization of SA at 45 °C using either 40:60 St:BA (StBA4060_45°C_40%SA, black squares) or 50:50 St:BA (StBA5050_45°C_40%SA, red circles) in the seed latex. (a) Overall conversions. (b) Instantaneous conversions. (c) Particle size evolution.

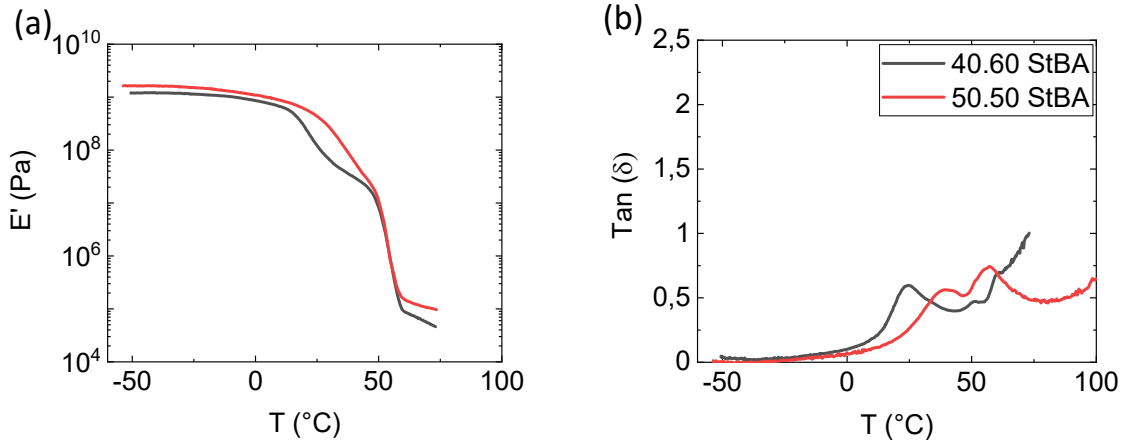

Figure S7. (a) Elastic modulus and (b) Tan (δ) as a function of temperature measured by dynamic mechanical thermal analysis of films cast from latexes synthesized by seeded semibatch emulsion polymerization of SA at 45 °C using either 40:60 St:BA (StBA4060_45°C_40%SA, black squares) or 50:50 St:BA (StBA5050_45°C_40%SA, red circles) in the seed latex.

Table S2. Young's modulus (E), yield stress (σ_y), stress at break (σ_{max}), elongation at break (ε_{max}) and toughness obtained from corresponding to the tensile stress–strain plots represented in **Figure 8**.

Sample	E (MPa)	σ_y (MPa)	σ_{max} (MPa)	ε_{max}	Toughness (MPa)
pSA_Em_30%pSA	8 ± 1	0.76 ± 0.07	*	*	*
pSA_Em_40%pSA	36 ± 2	1.50 ± 0.01	1.60 ± 0.07	7.7 ± 1.3	11.40 ± 1.95
pSA_Em_50%pSA	49 ± 7	1.93 ± 0.22	1.85 ± 0.26	6.4 ± 1.1	9.95 ± 2.21

*No sample breakage in the experimental strain range

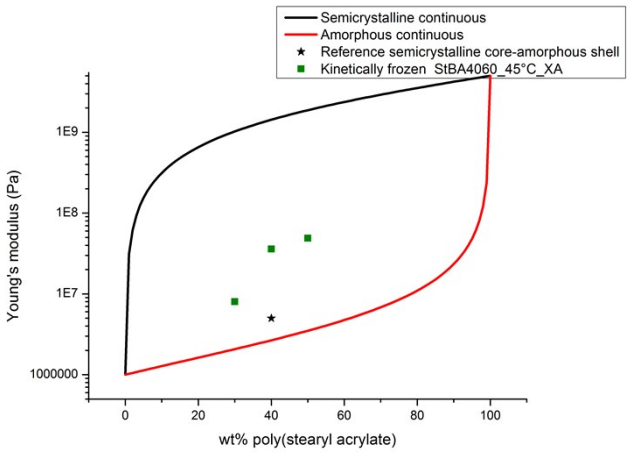

Figure S8. Comparison of the experimental results obtained in this work with the expected Young's modulus based on the Kerner equation assuming that the amorphous phase is continuous (red line) or the amorphous phase is present in discrete domains (black line).